



Characterization and recycling of lithium nickel manganese cobalt oxide type spent mobile phone batteries based on mineral processing technology

Ilyas Emir Çuhadar¹ · Fulya Mennik² · Nazlım İlkyaz Dinç² · Alim Gül² · Fırat Burat²

Received: 23 January 2023 / Accepted: 22 March 2023 / Published online: 31 March 2023
© The Author(s), under exclusive licence to Springer Nature Japan KK, part of Springer Nature 2023

Abstract

The unprecedented increase in mobile phone spent lithium-ion batteries (LIBs) in recent times has become a major concern for the global community. The focus of current research is the development of recycling systems for LIBs, but one key area that has not been given enough attention is the use of pre-treatment steps to increase overall recovery. A mechanical process combined with gravity, magnetic separation, and flotation was developed to recover metals and plastics. The results of the enrichment experiments in the coarse fraction showed that plastics with natural hydrophobicity could be obtained by reverse flotation. In the presence of hydrogen peroxide, sulfuric acid leaching was subjected to the black mass for recovering Li, Co, Ni, and Mn. The dissolution conditions were optimized by changing leaching parameters. The dissolution efficiencies of 96% Co, 94% Ni, 95% Mn, and 98% Li were achieved with 2 M H₂SO₄ concentration, 60 °C temperature, 2 h leaching time, and 40 g/L H₂O₂ dosage. In the precipitation step, NaOH was added to the leachate to increase the pH, and Co and Ni were partially separated from Mn at pH 7.7. The proposed flowsheet is basic and highly effective for the complementary recycling of components in Li-ion batteries.

Keywords Mobile phone lithium-ion battery · Recycling · Physical · Flotation · Leaching

Introduction

The increase in environmental concerns and collective awareness has led producers and consumers to sustainable and renewable energy sources to reduce the need for fossil fuel resources [1]. LIBs lead the global mobile phone market by a clear margin due to their attractive properties such as high energy density, longer life, size, and weight. LIBs have emerged as the best alternative in the range of energy storage products used in the consumer electronics (CEs) and electric vehicles (EVs) industries. Since mobile batteries have an approximate life of 3 years, they enter the recycling cycle faster than EVs with an average service life of 10 years [2,

3]. As the number of mobile phones continues to increase, so will the number of spent LIBs (S-LIBs) that need to be recycled [4–7].

LIBs are classified according to the content of the cathode material. LIBs used for portable energy storage generally include LCO (lithium cobalt oxide), NMC (lithium nickel manganese cobalt oxide), LFP (lithium iron phosphate), and NCA (lithium nickel cobalt aluminum oxide) based high-capacity cells. Due to the high cost, limited availability, and safety issues of cobalt, it cannot be considered a sole candidate in battery manufacturing. Li (Ni, Mn, Co) O₂-based batteries are entering the electrical-electronics and automotive application market to a large extent [8]. A typical LIB consists of an Integrated Circuit (IC) chip, a plastic or steel case, and a unit cell. The unit cell consists of a cathode, an anode, an organic separator, and an organic electrolyte. The active mass (also referred to as black mass or battery powder) contains cathode (Li, Co, Mn, Ni), anode (graphite), and the electrolyte (organic solvent containing dissolved lithium salts) powder, usually with a particle size of 0.8–0.1 mm. The cathode electrode is produced by pasting active cathode materials, carbon conductive additives,

✉ Fırat Burat
buratf@itu.edu.tr

¹ Exitcom Recycling Company, Çepni District, Suadiye Bağdat Street, No: 40, Kartepe, 41175 Kocaeli, Türkiye

² Mineral Processing Engineering Department, Faculty of Mines, Istanbul Technical University, Maslak, 34467 Istanbul, Türkiye

and binder (polyvinylidene fluoride or PVDF) on Al foil. Graphite and a binder are also spread on Cu foil to produce the anode electrode. According to Zhang et al., typical LIBs contains (by wt.) 7% Cu, 15% Al, 16% plastic, 41% active cathode material, 3% Ni, 16% graphite, and 7% electrolyte [9]. Metal concentrations in LIBs are often higher than those found in natural ores. In addition, S-LIBs contain a particular amount of heavy metals and toxic organics that can pose possible threats to the environment. Sustainable recycling of valuable materials in these batteries can be achieved through the application of mineral processing technologies, thus avoiding the negative effects of landfilling and incineration methods and providing critical material supply.

An integrated LIBs recycling process requires a range of applications involving all physical and chemical processes. Before chemical treatments are applied in the final stage, it is essential to select pretreatments based on mineral processing principles to separate valuable materials and remove contaminants [10]. If mechanical separation processes are not applied properly, the electrode foils and residues of the separators easily contaminate the black mass. Thus, metals and nonmetals with different behaviors in black mass may cause many critical issues such as loss of selectivity and recovery during the chemical process [11]. Collected and stored S-LIBs must be fully discharged to prevent possible explosions and fires before mechanical and chemical processing. The comminution process is required to peel off and remove the black mass from Cu and Al electrodes [12–14]. In general, coarse (Cu, Al, Fe, Ni, and plastics) and fine (black mass) liberated fractions are easily separated by a screen with a 0.3 mm aperture after gradual size reduction, and the black mass used in the dissolution process is not contaminated by these metals [15, 16].

The most valuable part of LIBs is the fine-size cathode active material, which contains critical and expensive metals such as Co and Li. Cu&Al foils, Fe&Ni casing metals, and plastics which accumulate in the coarse fraction as a result of mechanical processes are the basic parts of each LIB cell. Therefore, S-LIBs are the premium secondary source for these metals. Due to the wide difference between the specific gravity of plastics and metals, they stand out as very good candidates for gravity enrichment [17, 18]. Ferromagnetic metals (Fe&Ni) in LIB-S can be effectively separated from diamagnetic Cu and Al particles using a suitable magnetic separator. The main purpose of the physical processes performed here is to provide a concentrated raw material for further chemical processes [19–21]. Froth flotation, which is preferred in the mineral processing industry, is used to separate fine-sized particles that cannot be easily concentrated by physical methods, according to the difference in surface properties [22, 23]. Hydrophobic plastic particles with less free surface energy compared to metals can be

separated from hydrophilic metals by flotation with the help of appropriate reagents [24].

Mechanical/heat treatment, chemical, and leaching processes are generally used to recycle critical metals in the fine fraction of S-LIBs. Hydrometallurgical approaches such as acid or alkali leaching, chemical precipitation, separation, and electrochemical recovery are mainly adapted to recycling processes [25]. The pyrometallurgical route, on the other hand, involves mixing S-LIB with reductant and fluxes and melting it at high temperatures. At the end of this process, transition metals such as Co are reduced to a metal alloy, while Li remains in the form of slag. Recovery of Li from slag by hydrometallurgical treatment requires proper pretreatment, such as roasting. The applicability of pyrometallurgy remains limited due to its high energy consumption, toxic gas emission generation, and loss of Li [26]. Bio metallurgy uses microorganisms to produce lixiviants that dissolve the elements in S-LIB. Although the approach turns out to be cost-effective and environmentally friendly, the problems of its application on an industrial scale are the biggest barriers to this process. In hydrometallurgical processes, which have significant advantages over pyrometallurgy in terms of environmental protection and energy saving, target metals are selectively dissolved from S-LIB with the help of lixiviants.

In several studies using inorganic acids, it has been reported that metals such as Co and Li can be leached from S-LIBs using HCl [27, 28], H₂SO₄ [29–32], and HNO₃ [33]. In addition, the dissolution behavior of various organic acids such as citric, oxalic, malic, and ascorbic has been studied by some researchers [34, 35]. However, the industrial application of these acids is limited due to their long-leaching kinetics [36]. When the data in the literature are examined, H₂SO₄ has a great effect on the dissolution of active cathode materials in LIBs and is inexpensive compared to other solvents and widely used in industry. Co and Li can be easily leached out from S-LIBs using dilute acid solutions, but a reducing reagent such as hydrogen peroxide (H₂O₂) is essential for high metal recovery efficiencies. Otherwise, concentrated acid solutions are essential to achieve acceptable dissolution rates. Chen & Ho [37] extracted 99.5% of Ni, 90% of Mn, and 98% of Co from NMC 111 type battery using H₂SO₄ as the leaching agent and H₂O₂ as the reducing agent at 70 °C, S/L 30 g/L, 2 mol/L H₂SO₄, and 10% vol H₂O₂. Takahashi et al. [38] managed to dissolve 91% of Co from an LCO battery using H₂SO₄ and H₂O₂ at a 1:5 S/L ratio, 240 min leaching time, and 50 °C leaching temperature. Meshram et al. [39] achieved 96.4% Ni, 87.9% Mn, and 91.6% Co dissolution efficiencies in their NMC battery leaching study using 1 mol/L H₂SO₄ as lixiviant and 0.75 mol/L NaHSO₃ as reductant. The pregnant leach solution (PLS) containing dissolved metals obtained after solid–liquid separation

is further separated and purified using precipitation, solvent extraction, and selective adsorption.

The recovery of cobalt from purified leach solutions by precipitation with ammonium oxalate was reported by Swain [40]. After recovering Co^{2+} and Ni^{2+} from leaching solutions by solvent extraction (SX) method, lithium is usually precipitated using Na_2CO_3 , CO_2 , or H_3PO_4 [41, 42]. Metals such as Co, Ni, Mn, Cu, Al, and Fe can be selectively extracted at pH 6.5 using the SX process, while Li remains in the solution. SX reagents such as Cyanex 272, Acorga 5640, and PC-88A are preferred for the purification of pregnant leach solutions of S-LIBs [43]. Another method used for the selective recovery of metals is selective adsorption. In their study, Wang et al. [44] dissolved Li, Co, and Ni from S-LIBs using $\text{NH}_3\text{-H}_2\text{O-NH}_4\text{HCO}_3$ solution in the presence of H_2O_2 , and then selectively adsorbed Li from the solution with the help of an Mn-type Li-ion sieve.

The hydrometallurgical method may also present some disadvantages, which may complicate the process of recovering metals from the PLS and increase the cost. A process with easy and cost-effective recycling conditions should be designed for the sustainable recycling of metals in S-LIBs. Mechanical treatment and pre-enrichment before metal leaching increase the recovery efficiency of the target metals and facilitate the purification process. The complementary recycling of metals from S-LIBs has not been extensively investigated. Therefore, in this study, the recovery of Li, Co, Ni, and Mn from the black mass, which was purified from contaminants by mechanical processing before leaching, was investigated using H_2SO_4 as a lixiviant and H_2O_2 as a reducing agent. To optimize the conditions for the dissolution of valuable metals, the effects of parameters such as acid concentration, temperature, time, and dosage of the reducing agent were examined. According to some literature sources, the most suitable method for the selective separation of the desired metal from the liquor at a certain pH is the use of an organic solvent. Although solvent extraction directly serves this purpose, the need for large investment costs, space, and the prices of consumables emerge as the biggest problem. Therefore, pH-dependent precipitation remains the best option for recovering metals from charged solutions, especially for small and medium-sized industries. It has been reported that using sodium hydroxide, Mn precipitates out of the solution as MnO_2 [45]. In this study, pH-sensitive precipitation of Co, Mn, and Ni from the PLS was achieved using NaOH.

Due to their heterogeneous and complex nature, the complete recycling technology of S-LIBs unfortunately remains at the laboratory scale. Moreover, the existing studies in the literature mostly benefited from the manual dismantling process, which has no place in large-scale production, in the preparation of active cathode materials for the dissolution process. To facilitate the design of this study on an industrial

scale, two-stage size reduction and classification processes were applied to discharged S-LIBs, and enrichment studies for foil metals (Cu&Al), plastics, and casing metals (Fe&Ni) were carried out by physical and physicochemical tests.

Experimental

Materials

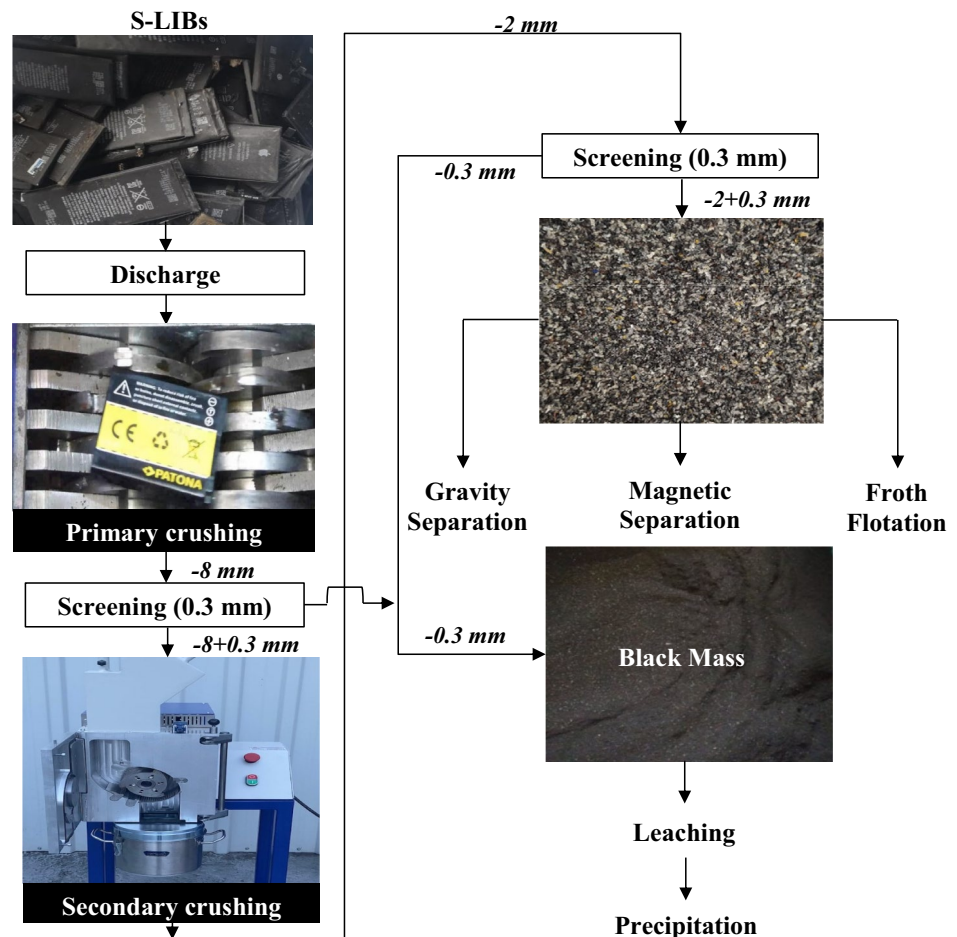
In experimental studies, NMC-type S-LIBs with a weight of approximately 40 kg containing active cathode materials such as Li, Co, Ni, and Mn in different models and brands were obtained from Exitcom Recycling Co. located in Kocaeli, Türkiye. In line with the basic operation of the process, the company carried out the primary crushing process using a four-shaft shredder immediately after the discharge process. Beneficiation studies were carried out using mechanical, physical, physicochemical, and chemical methods. To design the flow diagram based on the experimental data, it is essential to provide the contents of the components. As a result of the classification process performed after the size reduction processes, there were obvious differences in physical appearance between the coarse and fine fractions (see Fig. 1). While the cathode, anode, binder, electrolyte, and separator materials forming the black mass passed in fine size, the coarse fraction consisting of laminated plastics, Cu and Al foils, and Fe&Ni containing casing metals remained on the sieve.

For coarse fractions, chemical analysis studies were carried out using the aqua regia acid digestion method. About 0.50 g of sample was added to the beaker with HNO_3 (5 mL, 69%), HCl (15 mL, 36%), and H_2O_2 (2 mL, 30%) and heated around 150 °C and kept for 12 h. The insoluble fraction was filtered out, and the filtrate was analyzed using Varian AA50-type atomic absorption spectroscopy (AAS). The chemical analysis of fine fraction (black mass) was also carried out by Inductively Coupled Plasma Mass Spectrometry (ICP) for Co, Li, Mn, Cu, Al, Fe, and Ni. The LECO elemental analyzer was used to determine the presence and concentration of carbon and sulfur. The analyses were repeated three times and the weighted averages were calculated. The flotation chemicals, MIBC (DOW Chemical Company), were used as frother. In the leaching experiments, H_2SO_4 and H_2O_2 were used as lixiviant and reducing agents, respectively. NaOH was chosen to precipitate metals from the leach liquor. All the chemicals used were analytical grade.

Comminution and characterization of the S-LIBs

As opposed to other batteries, lithium metal frequently explodes in the recycling process when exposed to air and mechanical shock [46]. Therefore, the batteries were

Fig. 1 The flowsheet of the recycling process for S-LIBs



completely discharged at the plant before the primary crushing. A pre-separation is required to reduce scrap volume, separate battery components, and selectively enrich valuable metals from the S-LIBs. Since this study covers not only the recycling of the active cathode and anode materials from the black mass by leaching, the enrichment of Cu, Al, Fe, and Ni in coarse-size fractions has been investigated using physical and physicochemical methods. The crushing and recovery operations need to be carried out in an automated machine process for commercialization purposes. In the leaching process with high acid concentration, the particles do not need to be ground very finely, however, the active cathode material covering the aluminum foil is difficult to peel off. Therefore, multi-stage crushing and classification were subjected to fully discharged S-LIBs as presented in Fig. 1.

Discharged S-LIBs were primarily fed to the double-shaft shredder. The output size of the shredder was adapted to 8 mm so that the anode and cathode plate materials (Cu and Al foils) were prevented from passing to fine grain sizes and contaminating the black mass. The crushed material was then sieved through a 0.3 mm screen to reserve the black mass for hydrometallurgical studies. Due to the

size and shape difference, materials such as plastics, foils, and casing materials remained on the over-screen and were subjected to secondary stage crushing using a four-blade cutting mill (RAM200 model manufactured by Rantek Co.) to bring them to a suitable size for the subsequent enrichment processes. The size of the replaceable curved sieve located in the lower section of the mill was chosen as 2 mm. The binders used to hold the cathode active materials on the substrate cause the battery powder to remain adhered, especially on aluminum surfaces. As a result of the second stage crushing, the remaining fine materials on the surfaces of the foils were peeled off. The fine fraction was screened below 0.3 mm and combined with the previously separated black mass in the primary stage comminution and classification. After gradual size reduction, the S-LIBs samples were characterized according to the particle size distribution (PSD) and chemical analysis. The PSDs of the products obtained as a result of comminution and classification were determined by dry sieve analysis. A laser analyzer, Mastersizer 3000 (Malvern Instruments) with Hydro MU adapter, was used to ascertain the PSD of the black mass.

Physical beneficiation studies

The shape and surface properties of the particles, the density, and magnetic and electrostatic differences between valuable and gangue materials directly determine the physical enrichment method to be applied. In the first part of the study, which was carried out using the coarse fraction, the focus was on the concentration of metallic values with high metal recovery rates and the removal of plastics with low metal contents. The specific gravities of Cu, Al, Fe, and Ni metals that present at high concentrations in the coarse fraction of S-LIBs are 8.9 g/cm^3 , 2.7 g/cm^3 , 7.8 g/cm^3 , and 8.6 g/cm^3 , respectively. On the other hand, the specific gravity of the plastics that mainly make up the waste matrix is around 1 g/cm^3 .

The large specific gravity difference between metals and plastics and the suitable particle size gap ($-2 + 0.3 \text{ mm}$) brought up the idea of using the shaking table because of its simplicity, ease of use, effectiveness, high capacity, environmentally friendly, and cheapness. In the gravity separation tests, a laboratory scale Wilfley-type shaking table with a surface of $80 \times 40 \text{ cm}$ was used. The heavy and light products accumulating in different separation zones according to particle density, size, and shape in the fluid medium on the table surface were separated using adjustable splitters. The test conditions are as follows: 10 L/min wash water, 2 mm stroke length, 300 cycles per min frequency, 3° lateral angle, 30 kg/h feed rate. The laboratory-type dry high gradient rare earth magnetic separator (REMs) with 4000 Gauss (G) magnetic field was conducted to separate ferromagnetic Fe and Ni from diamagnetic Cu and Al particles. In addition, low gradient intensity wet band magnetic separator (WBMS) was used to capture and separate the iron contained in the black mass before leaching.

Reverse flotation studies

The non-wetting surface properties of plastics and the hydrophilic nature of metals have highlighted the flotation method as an environmentally friendly and economic solution for the enrichment of coarse-sized S-LIBs. Pre-treatments to make coarse-sized materials ($-2 + 0.3 \text{ mm}$) suitable for flotation tests were described in our previous study [47]. The surface-cleaned coarse fraction was fed into a 1.5 L self-aerated Denver-type flotation equipment. No pH adjuster was used due to environmental concerns and the natural pH value of the pulp was measured as 8.3. The particles were contacted with the frother (MIBC) for 5 min with a 1200 rpm impeller speed, then the air valve (3 L/min air flow rate) was opened and the plastic particles with high hydrophobic properties were separated by floating for 3 min.

Acid leaching studies with H_2SO_4

The dissolution studies of battery powder containing active cathode materials such as Co, Li, Ni, and Mn were performed in sulfuric acid media. To dissolve the metallic values in the black mass, H_2SO_4 was poured into the distilled water at the determined concentrations and H_2O_2 was used as the oxidizing agent. The black mass weighing 10 g was added to a temperature-controlled 0.6 L glass reaction container. The stirring rate was set to approximately 300 rpm and the black mass weighing 10 g was added to 200 mL of leaching liquor (liquid-mass ratio of 20 mL/g). After leaching, each sample was vacuum filtered and the filtrate was analyzed using AAS. The dissolution efficiency of metal components is defined as the ratio of the component amount in the solution water to the amount in the feed material.

Precipitation tests with NaOH

After determining the optimum leaching conditions that achieve the highest extraction rates, the metals were precipitated using NaOH. NaOH remains the best choice, as it is a strong base reagent that allows working with small volumes of solution and is widely used in industrial applications. Precipitation tests were performed using a 1000 ml glass reactor. The PLS was put down in the reactor and NaOH was dripped slowly and in a controlled manner. The pH of the solution was continuously monitored and samples were taken, filtered, and analyzed for a given pH (range 4–11).

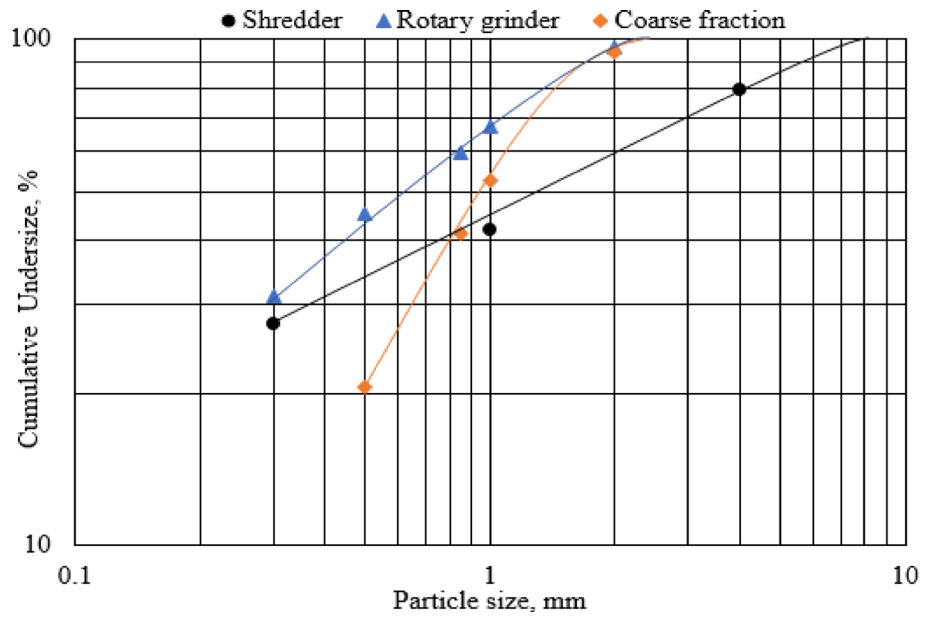
Results and discussions

Characterization of the S-LIBs

In the characterization studies, firstly, the PSD of the representative S-LIBs sample, which was crushed into different sizes as a result of the comminution and classification processes, was investigated, and then the metal contents in coarse and fine fractions were identified. PSD curves of the S-LIBs sample after the primary (shredder), secondary (rotary grinder) crushing, and classification ($-2 + 0.3 \text{ mm}$) are illustrated in Fig. 2.

The d_{80} and the d_{50} sizes of the shredded material were found as 4.1 mm and 1.4 mm, respectively. $-4 + 1 \text{ mm}$ is the most dominant fraction with a share of 37.1%. After the second stage of crushing, the d_{80} and the d_{50} sizes decreased dramatically to 1.4 mm and 0.6 mm, respectively. The amount of material below 0.3 mm increased by approximately 4% at the end of the second stage size reduction. This difference is due to the anode and cathode active materials that could not be completely stripped from foils in the first stage comminution process. The d_{80} and the d_{50} sizes

Fig. 2 Particle size distribution curves of the products after the comminution and classification



of the black mass were determined by the laser particle size analyzer as 108 and 47 microns, respectively. As a result of the classification process after the second stage size reduction process, a coarse fraction (68.8% w.t. of the total feed)

consisting of Cu foils, Al foils, battery casing, and plastics was obtained. As seen in Fig. 3, metal and plastic materials retained their sheet-like structure in the comminution process based on shear and compression forces. Moreover,

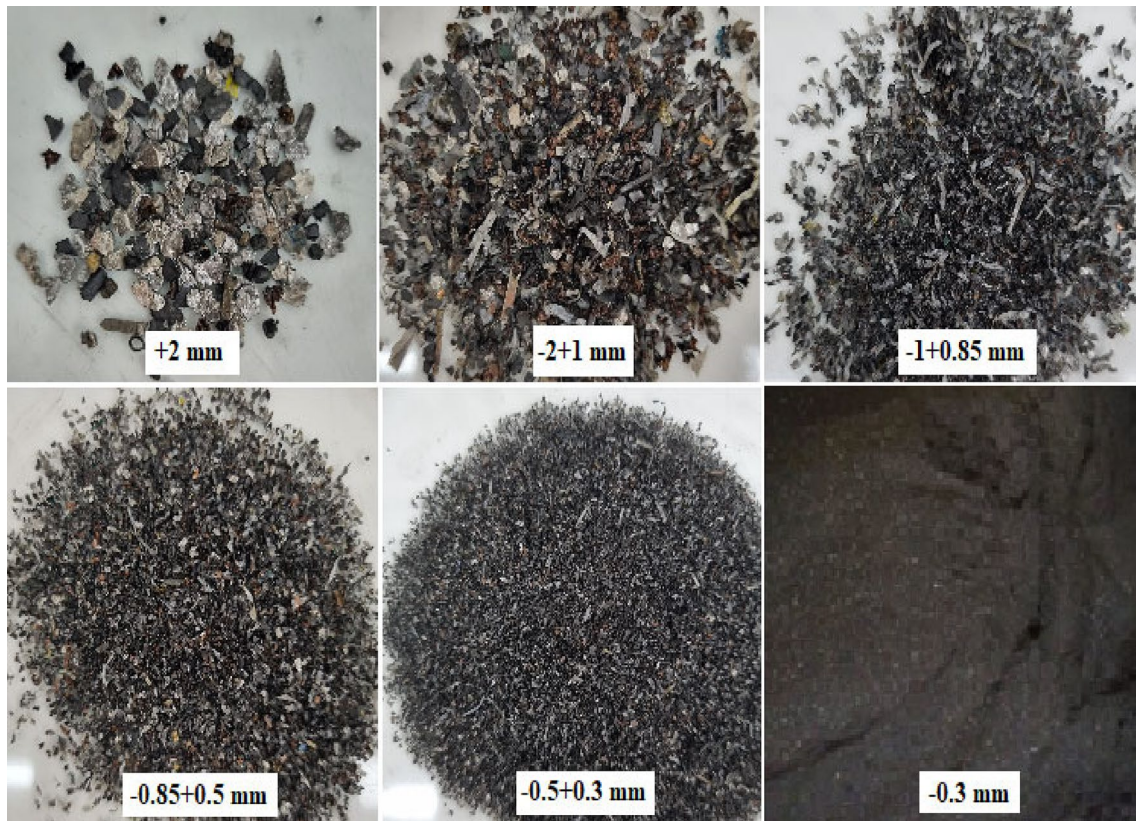


Fig. 3 Macroscopic images of the fractions after comminution and classification

plastics, foils, and casing metal particles were observed as single grains. The common shape characteristic of these components, which make up the coarse fraction, provides a very important advantage in metal–plastic and metal–metal separation in the enrichment processes. While the coarse fraction was evaluated in physical and physicochemical beneficiation studies, fine-size black mass (31.2% w.t. of the total feed) was used in the dissolution tests.

The results of chemical analyses indicated that the representative sample contained 14.98% Cu, 13.01% Al, 7.56% Fe, and 3.08% Ni. In the coarse fraction, the total content of four metals was 50.4%, however, it dramatically decreased to 12.7% in the black mass. In addition, the coarse fraction mostly consists of Cu and Al since they are the coating metals of the active substances. Because they are produced in foils, these two metals are concentrated in sizes above 0.3 mm, thus their amount in the black mass decreases dramatically. Fe and Ni, on the other hand, took a flat shape as a result of comminution and remained over-screen. As seen in Fig. 4, an average of 90% of these metals were distributed in the coarse fraction and their contents increased to 20.52% Cu, 15.57% Al, 10.22% Fe, and 4.09% Ni. On the other hand, the metal contents of the fine fraction (the black mass) dropped dramatically to 2.76% Cu, 7.38% Al, 1.7% Fe, and 0.85% Ni. In addition, powdered active battery materials contain 23.46% Co, 1.39% Li, 18.95% Mn, and 42.7% carbon (from graphite).

Li-ion battery recycling methods aiming to recover metals based on characterization results consist of the following

steps: (1) the comminution process and classification, (2) removal of plastics in the coarse fraction from metals by gravity and froth flotation, (3) separation of the ferrous fraction from non-magnetics by magnetic separation, (4) dissolution of metals in the black mass using $H_2SO_4 + H_2O_2$, and finally (5) recovery of Co, Ni, and Mn in the PLS by NaOH precipitation.

Physical beneficiation studies

In the first stage of the physical enrichment studies, the shaking table test was applied to a previously comminuted and classified coarse fraction (− 2 + 0.3 mm). The contents and distributions of metals are given in Table 1. According to the results of the gravity separation, a heavy product with a weight of 51.0% was obtained with 20.12% Cu, 24.04% Al, 15.93% Fe and 7.28% Ni contents, and the total content of four metals was around 67%. The light product weighing approximately 22.7% by the feed, consisting mostly of coarse plastic and fine metal particles, was discarded with the contents of 5.14% Cu, 2.44% Al, 3.73% Fe, and 0.22% Ni. Since Al is the metal with the lowest specific gravity among the metals in the coarse fraction, some Al particles escaped to the separation zone in the middle of the table. The relatively high iron content in the same product indicates that the particles could be in the form of Fe&Al alloys. Copper foils, which are found as liberated particles, were caught by the drag forces of the water flowing in the fluid layer due to their shape feature and mixed especially with the middlings. In addition, casing metals have greater thicknesses than Cu foils, so the recovery rates of Fe and Ni are more than 78%. The total content of metals in the light product is 11.5%, and the total metal loss is only 5.2%. The main purpose of gravity separation studies was to remove free and large plastic particles and to obtain a heavy fraction with high metal content and recovery, however, due to the difficulties arising from the shape of the particles, especially foil-type metals have moved to middling and light products [48]. To effectively recover these metals, the particles could be given a spherical shape with proper size reduction equipment such as an impact crusher. However, the most critical challenge here is that different metals will come together to

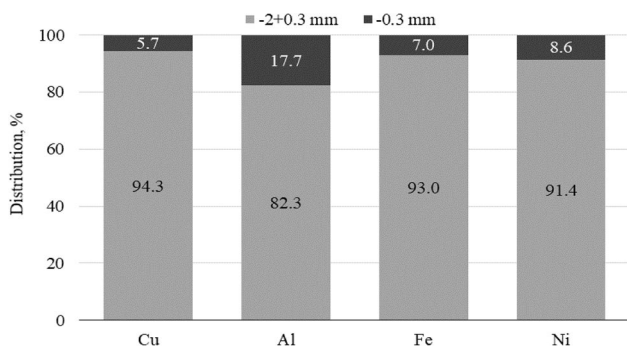


Fig. 4 The distributions of metals at coarse and fine fractions

Table 1 Metal contents and distributions of the products after gravity separation

Products	Amount, %	Cu		Al		Fe		Ni	
		C, %	D, %	C, %	D, %	C, %	D, %	C, %	D, %
Heavy	51.0	20.12	50.0	24.04	77.9	15.93	78.9	7.28	89.6
Middlings	26.3	34.64	44.4	11.12	18.6	5.02	12.8	1.45	9.2
Light	22.7	5.14	5.7	2.44	3.5	3.73	8.2	0.22	1.2
Total	100.0	20.54	100.0	15.74	100.0	10.29	100.0	4.14	100.0

C content, D distribution

form larger grains and the selectivity will decrease in the further enrichment process.

Magnetic separation was subjected to the coarse fraction as another physical enrichment option. The main purpose here was to separate ferrous metals from diamagnetic Cu and Al particles. As seen in Table 2, a magnetic product weighing about 32.6% by the feed was obtained with 30.68% Fe and 12.21% Ni contents. As expected from magnetic separation, ferromagnetic Fe and Ni were successfully obtained with recovery rates of 97.9% and 96.6%, respectively. Although the recovery percentages of Cu and Al are high in the non-magnetic product, their contents couldn't be reduced below 4%. Due to the static electricity charge formed on the surfaces of Cu foils and their layered shape that allows sticking to the drum, some Cu and Al particles were misplaced and transported to the rear compartment where the magnetic product was taken. The iron particles were easily separated from the diamagnetic metals, and the Fe and Ni contents dropped to 0.32% and 0.21%, respectively. The insulating plastic particles that remained in the non-magnetic product could be removed from the conductive Cu and Al particles using an electrostatic separator. Then, Cu and Al particles might be taken as separate concentrates by subjecting them to an Eddy Current separator.

Reverse flotation studies

The plastic particles used in LIBs have been converted to a laminated shape after the comminution process. Besides particle shape characteristic, which is positive for reverse flotation, their natural hydrophobic properties and low specific gravities create a great advantage over metals with wettable properties and high specific gravity. Plastics, which have superior flotability compared to hydrophilic metal particles, were separated by the reverse flotation method with the help of a frother agent (MIBC). The optimum parameters were determined as a frother dosage of 500 g/t, a particle size of $-2+0.3$ mm, an impeller speed of 1200 rpm, a condition time of 5 min, and a flotation time of 3 min.

Fadel et al. [49] found the contact angle value of pure PET to be 78.9° , which indicates the hydrophobic property of the polymer. Saneie et al. [50] determined the contact angles of the unconditioned Cu and Al foils in 18,650-type

rechargeable S-LIBs as 39.9° and 43.9° , respectively. This significant difference in contact angle between plastics and metals directly proves the flotation success of plastics. The cumulative weight of the floated plastics systematically increased to approximately %99 with a frother dosage of 500 g/t. As shown in Fig. 5, about 17.1% weight of the total feed was floated with 1.46% Cu, 2.01% Al, 0.41% Fe, and 0.15% Ni contents. Especially fine sized and laminated metal particles did not sink in the pulp despite their high specific gravity and were carried to the floating product. However, the total metal loss is quite low (only 1.4%). Flotation test results have proven that the plastic particles that make up the waste can be effectively recovered in the reverse flotation process. The rough metal concentrate (82.9% by wt.), which did not float in plastic flotation and remained in the cell assay 24.56% Cu, 18.50% Al, 12.31% Fe and 4.95% Ni. As noted in our previous study, magnetic particles in the coarse metallic fraction after plastic flotation can be captured using REMs, and Cu particles in the non-magnetic fraction can be recovered by the flotation method in the presence of suitable collectors (potassium amyl xanthate (KAX) and Aerophine 3418A) [47]. Another suitable approach would be to feed the non-magnetic product to an electrostatic or Eddy current separator for Cu–Al separation.

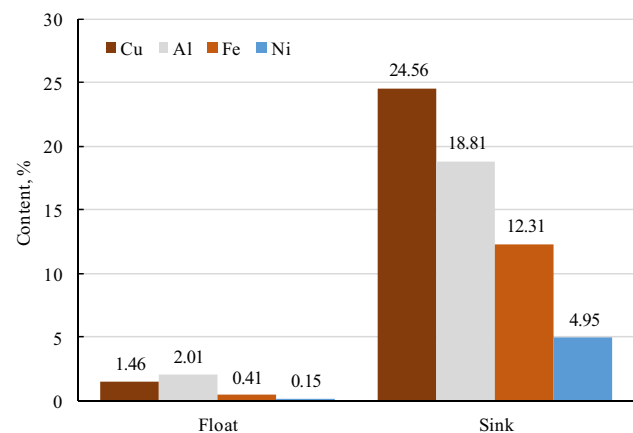


Fig. 5 The metal contents of reverse flotation products

Table 2 Metal contents and distributions of the products after magnetic separation

Products	Amount, %	Cu		Al		Fe		Ni	
		C, %	D, %	C, %	D, %	C, %	D, %	C, %	D, %
Magnetic	32.6	4.89	7.8	4.02	8.4	30.68	97.9	12.21	96.6
Non-magnetic	67.4	28.15	92.2	21.22	91.6	0.32	2.1	0.21	3.4
Total	100.0	20.57	100.0	15.61	100.0	10.22	100.0	4.12	100.0

C content, D distribution

Reductive acid leaching studies

In the leaching process, the main goal is to achieve the highest metal dissolution in the PLS under optimum conditions (low energy, high efficiency, low reagent consumption, and high solids percentage) while keeping the content of other impurities at a minimum. During the production phase of LIBs, an iron plate is placed on the poles to increase the resistance of the battery case. As a result of gradual crushing processes, the ferrous fraction dispersed to the fine fraction causes both capacity increase and difficulties that may arise during the leaching process. For this purpose, before the dissolving of metals, the black mass was fed to REMs to capture Fe particles. As a result of magnetic separation, Fe was removed with a recovery rate of about 95%, and its content in the non-magnetic product was decreased to 0.08%. Dissolution experiments were carried out while charging a certain amount of black mass in the absence/presence of a reducing agent (H_2O_2) in sulfuric acid solution. Temporary exploratory tests were conducted to obtain the most adequate L:S ratio (20 mL/g) and stirring speed (300 rpm) to dissolve the cathode materials of Li-ion batteries. The effects of varied process parameters such as sulfuric acid concentration (1–4 M), reaction temperature (25–80 °C), leaching time (60–150 min), and concentration of reductant (0–50 g/L) on the dissolution of Li, Co, Ni, and Mn were investigated. H_2SO_4 concentrations of 1, 2, 3, and 4 M were tested by keeping the H_2O_2 amount (10 g/L) and temperature (80 °C) constant during the leaching duration of 120 min. The effects of acid concentration on the amount of Co, Ni, Mn, and Li extracted from the black mass are illustrated in Fig. 6.

The results indicate the dissolution efficiency of 68.7% Co, 78.7% Ni, 86.9% Mn, and 61.4% Li at 1 M H_2SO_4 concentration. The increase in acid concentration facilitates metal leaching due to the increase of reagents in the reactive system. The acceleration in Co, Ni, and Li dissolution

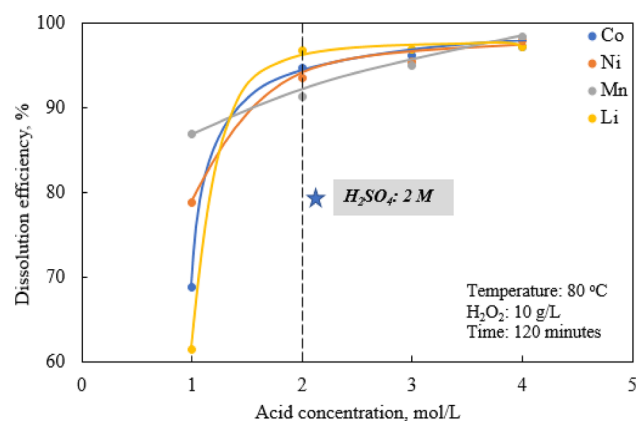


Fig. 6 The effect of acid concentration on the dissolution efficiency of Co, Li, Ni, and Mn

rates slowed down after 3 M, however, Mn continued to increase linearly. Confirming the findings of Meshram et al. [39], the addition of sulfuric acid eased the reaction and increased the dissolution rates of metals. Although the dissolution efficiency can be improved especially for Co, Ni, and Mn at 3 M acid concentration, 2 M H_2SO_4 concentration was deliberately chosen for process economy and for further studies to emphasize the effect of other leaching parameters on increasing recovery.

As another important parameter, the effect of leaching temperature on the dissolution of valuable metals was investigated using 2 M H_2SO_4 , 120 min leaching time, and 10 g/L H_2O_2 concentration. The results in Fig. 7 show that the temperature is statistically significant as the leaching parameter. Approximately 76% Co, 79% Li, 51% Ni, and 84% Mn were extracted at room temperature (25 °C) and the increase in the temperature dramatically improved the leaching reaction. Since the dissolution reaction of metals is an endothermic process, the average kinetic energies of the molecules increase with temperature, which causes more frequent and energetic collisions, increasing the rate of dissolution [51].

Parallel to the findings of Pinna et al. [52] and Kang et al. [53], since H_2O_2 decomposes to H_2O and O_2 at temperatures above 80 °C, the dissolution yields remained constant from this point forward. The effect of increased ambient temperature on the solubility of Co and Mn is much lower than that of Ni. It is seen that the dissolution rate of Mn slowly increases with increasing temperature from 25 to 80 °C. Increasing the temperature of the pulp results in more energy consumption and therefore higher cost. Therefore, the temperature value that provides low energy consumption and high dissolution efficiency should be accepted as the optimum parameter. 60 °C was accepted as the optimum leaching temperature value since there was no significant difference in the dissolution efficiency at 80 °C. The effect of time (0–150 min) on the dissolution efficiency of metals

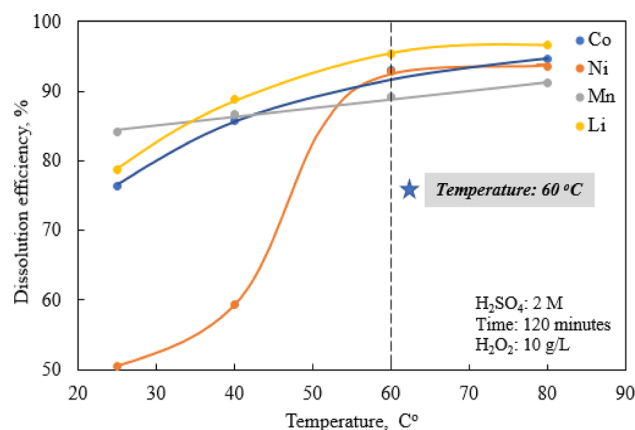


Fig. 7 The effect of leaching temperature on acid leaching of Co, Li, Ni, and Mn

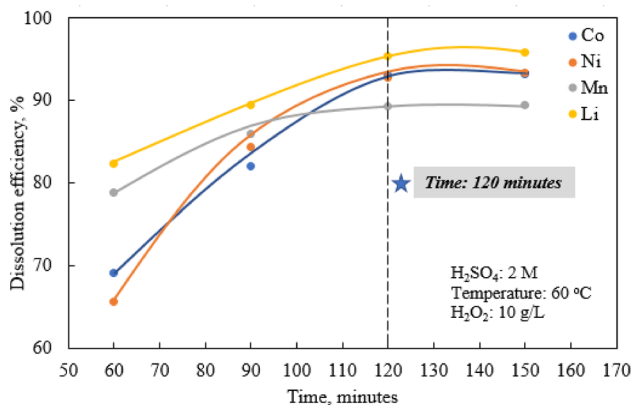


Fig. 8 The effect of leaching time on acid leaching of Co, Li, Ni, and Mn

was investigated using 2 M H_2SO_4 concentration, 60 °C temperature, and 10 g/L H_2O_2 dosage.

The increase in the reaction time improved the extractions of Co, Li, Ni, and Mn indicating that the contact time between the reactants favored the dissolution reaction (Fig. 8). It was also observed that the dissolution rate steadily increased and leaching saturation was achieved within 120 min. Co and Ni exhibited similar dissolution behavior over time and the rate of leaching for Mn was the lowest. Dissolution efficiencies of more than 89% were obtained for these metals after 120 min. It is worth noting that after 90 min of dissolution time, more than 80% dissolution is achieved and this will be beneficial if the process is to be accelerated. Since the metal dissolution efficiencies at 160 min of leaching time were almost the same, the optimum leaching time was accepted as 120 min.

To examine the effect of reductant dosage on the dissolution of metals, the dosage of H_2O_2 was changed in the range of 0–50 g/L. Previously determined parameters maintained during the leaching contain: H_2SO_4 concentration of 2 M, 60 °C of temperature, and 120 min of leaching time. As shown in Fig. 9, the dissolution rates of Co and Mn were significantly promoted when H_2O_2 was added to the leaching solution. The results indicated that the dissolution efficiency of metals increases from 68.2% to 96.4% for Co, 84.4% to 95.1% for Ni, 50.2% to 94.9% for Mn, and 86.5% to 98.6% for Li in the absence and presence of the reducing agent at 50 g/L of H_2O_2 concentration, respectively. It can be concluded that relatively high leaching of Ni and Li can be achieved at low acid concentrations and in the absence of a reducing agent. Because the chemical bond between cobalt and oxygen is very strong, acid dissolution of lithium cobalt oxide is quite a challenge.

Oxygen emerging from the decomposition of hydrogen peroxide helps dissolution by accelerating the reaction and converting Co^{3+} to Co^{2+} and Mn^{4+} and Mn^{2+} [54–56]. The

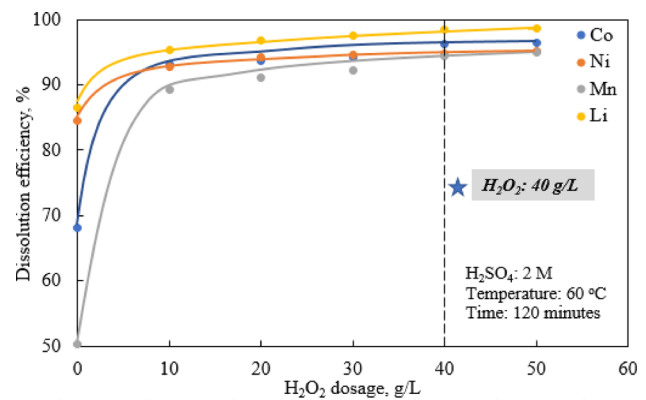
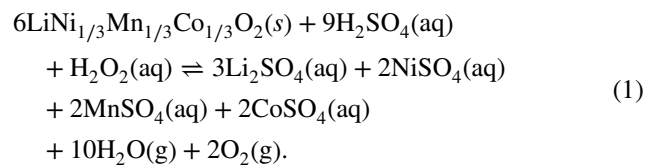


Fig. 9 The effect of hydrogen peroxide amount on metal dissolution efficiency

following reaction stoichiometry (1) shows that nickel-manganese-cobalt-lithium oxide battery ($\text{LiNi}_{1/3}\text{Mn}_{1/3}\text{Co}_{1/3}\text{O}_2$) reacts with H_2SO_4 and produces nickel, manganese, cobalt, and lithium sulfates [37].



Hydrogen peroxide can help dissolve cobalt and manganese by reducing them to lower oxidation states, while also promoting the dissolution of lithium due to its association with the same oxide phases as cobalt and manganese. Since the dissolution of metals was largely completed at 40 g/L H_2O_2 and a further increase in H_2O_2 dosage did not significantly improve the recovery rates this value was accepted as optimum. Finally, it can be concluded that the most important variables in the dissolution of active cathode materials from Li-ion batteries for the studied operating conditions are H_2SO_4 concentration, temperature, H_2O_2 concentration, and time, respectively. A further supporting leaching test was carried out by keeping the optimized parameter values (2 M H_2SO_4 concentration, 60 °C leaching temperature, 120 min leaching time, 40 g/L H_2O_2 dosage). The final leaching experiment gives an almost full recovery of active cathode materials (96.0% Co, 94.5% Ni, 95.4% Mn, and 98.7% Li) from S-LIBs. The carbonaceous material does not dissolve in the acid solution, but instead floats on the solution and is separated in the cake during filtration.

Precipitation tests with NaOH

The precipitation process was carried out to recover metallic values in hydroxide forms from the PLS. The pH value of the filtrate from solid–liquid separation was measured

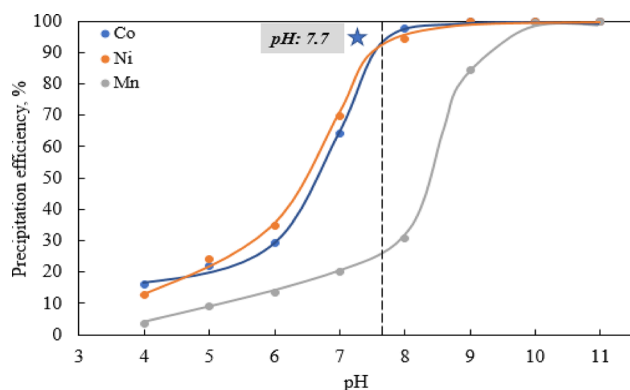
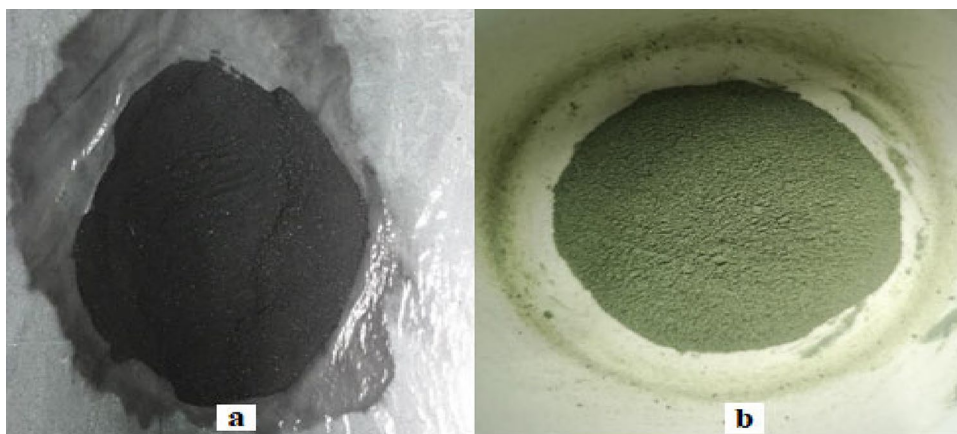


Fig. 10 The precipitation curves of Co, Ni, and Mn at different pH values

as 0.83. Sodium hydroxide was dissolved in deionized water and modified the pH value. The precipitation curves of Co, Ni, and Mn are presented in Fig. 10. The pH of the medium increases with the addition of NaOH to the solution medium. Because of their similar chemical properties, Co and Ni began to precipitate at almost the same pH value (around 6). This means that Co and Ni cannot be precipitated separately in the form of hydroxide. While the precipitation of Co and Ni is completed at about pH 7.7, Mn starts to precipitate dramatically around pH 8. Therefore, the pH value can be adjusted between 7.7 and 8 for the selective precipitation of Co and Ni from Mn. To precipitate Li, its concentration in the PLS must be above 20,000 ppm, therefore, Li could not be precipitated in one batch. Li recovery will be possible with a more saturated solution and gradual crystallization. The precipitated material with controlled pH increase was subjected to solid–liquid separation, then the filter cake was dried at 75 °C for about 15 h and removed from its moisture. Figure 11 shows the black mass and the precipitated cathode material.

Fig. 11 The black mass (a) and the precipitated cathode material (b)



Proposed flowsheet for S-LIBs recycling

In line with the information obtained from the characterization and beneficiation studies, a flowchart was generated for the recycling of S-LIBs components (Fig. 12). After the discharging process, the S-LIBs sample was fed to two-stage comminution and 31.2% by weight of fine material (black mass) was removed from coarse fraction using a 0.3 mm sieve. The coarse fraction weighing 68.8% of the total feed was subjected to gravity and magnetic separation tests as two different physical enrichment method options. In shaking table experiments, a heavy fraction with a 35.1% by weight to the total was produced with 20.12% Cu, 24.04% Al, 15.93% Fe, and 7.28% Ni contents. A light product assaying 5.14% Cu, 2.44% Al, 3.73% Fe, and 0.22% Ni contents was discarded. In the gravity separation, an increase was observed in the content of Cu and Al due to their plate-shaped characteristics. Here, the misplaced metals, Cu and Al, could be separated according to their electrostatic properties. Magnetic separation has been very effective in the recovery of ferrous materials with high content and recovery. Although the Cu and Al contents in the magnetic product are still high, they can be recaptured in a second cleaning step. The Fe and Ni contents in the non-magnetic product are quite low, therefore electrostatic separation can also be considered in this product for the selective production of Cu and Al metals.

The coarse fraction was transferred to the flotation cell as a physicochemical process option and plastic particles were efficiently separated using 500 g/t of MIBC. It is strongly recommended to apply electrostatic or an eddy current separation to the non-magnetic product for separating Cu and Al particles. The black mass containing critical and expensive metals was fed to the wet magnetic separator to remove the problematic iron during the leaching. While precious metals were taken into solution by reductive acid leaching, graphite with about 96% C content was obtained in the filter cake. As

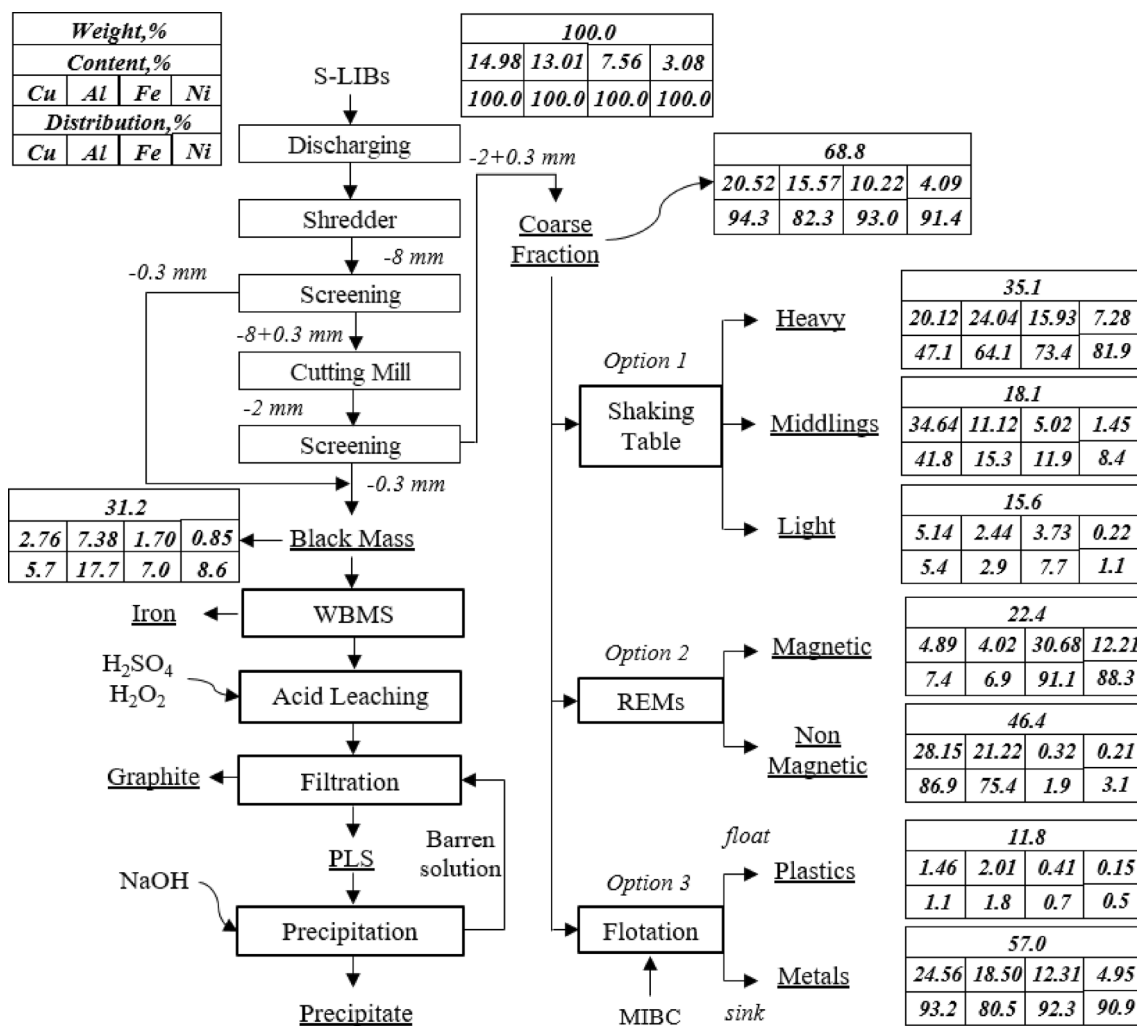


Fig. 12 Proposed flowchart for recycling of S-LIBs

a result of precipitation with NaOH, around pH 7.7, 94% of Co and Ni precipitated as hydroxide, and only 25% of Mn.

Conclusions

Mechanical separation of the black mass forming the active cathode–anode materials and subsequent recovery of Li, Co, Ni, and Mn by the hydrometallurgical procedure is the primary objective of this original study. The recovery of high-priced cathode active materials seems much more attractive, however, Cu–Al foils, Fe–Ni casing metals, and plastics, which are the basic parts of LIBs, are also a superior source for recovery. For this reason, a viable flowchart including mechanical, physical, and physicochemical steps is added for the comprehensive recycling of coarse-size S-LIB components. Gravity and magnetic separation processes alone were not sufficient to produce the final metallic concentrate. Since the material has a heterogeneous structure, it is necessary to

perform separation processes in the form of different combinations of more than one stage. The results showed that the plastics could be easily separated from the metal mixture by the conventional flotation method.

As a result of decreasing the complexity of LIBs structure and obtaining selective metallic concentrates, a capacity increase and complexity decrease can be achieved in the further leaching and refining process. For this purpose, in leaching studies using battery powder, 2 M of H₂SO₄ concentration, 60 °C of leaching temperature, 2 h of leaching time, and 40 g/L H₂O₂ dosage were determined as optimum conditions. Despite some challenges, the recovery of foils and ferrous fractions from spent LIBs can be achieved through economical and environmentally friendly mineral processing techniques. According to the results of this study, these methods could be adapted to other similar and different types of batteries used in CEs or Evs. Finally, it is strongly recommended that pilot-scale experiments and economic analysis be performed before commercialization.

Acknowledgements The present study is based on the results of the graduate and undergraduate thesis conducted at Istanbul Technical University. The authors sincerely thank the Mineral Processing Department of Istanbul Technical University for providing laboratory equipment and analysis for this research. We would like to thank Exitcom Recycling Co. for supplying the S-LIB samples. We are grateful to Rantek Co. for their support in crushing battery samples to fine size by cutting mill.

Author contributions FM, NİD, İEÇ, and FB contributed to the investigation, methodology, and experimental design. FB and AG are involved in supervision, validation, writing-original draft, review, and editing.

Data availability The authors confirm that the data supporting the findings of this study are available at <https://doi.org/10.1007/s10163-023-01652-5>.

Declarations

Conflict of interest On behalf of all authors, the corresponding author states that there is no conflict of interest.

References

- Kaya M (2022) State-of-the-art lithium-ion battery recycling technologies. *Circ Econ* 1:100015. <https://doi.org/10.1016/j.cec.2022.100015>
- Ebin B, Petranikova M, Ekberg C (2018) Physical separation, mechanical enrichment and recycling-oriented characterization of spent NiMH batteries. *J Mater Cycles Waste Manag* 20:2018–2027. <https://doi.org/10.1007/s10163-018-0751-4>
- Chen X, Ma H, Luo C, Zhou T (2017) Recovery of valuable metals from waste cathode materials of spent lithium-ion batteries using mild phosphoric acid. *J Hazard Mater* 326:77–86. <https://doi.org/10.1016/j.jhazmat.2016.12.021>
- Celep O, Yazıcı EY, Devenci H, Dorfling C (2022) Recovery of lithium, cobalt and other metals from lithium-ion batteries. *Pamukkale Univ J Eng Sci*. <https://doi.org/10.5505/pajes.2022.98793>
- Grey CP, Tarascon JM (2017) Sustainability and in situ monitoring in battery development. *Nat Mater* 16:45–56. <https://doi.org/10.1038/nmat4777>
- Choubey PK, Chung K, Kim M, Lee J, Srivastava RR (2017) Advance review on the exploitation of the prominent energy-storage element Lithium. Part II: From sea water and spent lithium ion batteries (LIBs). *Miner Eng* 110:104–121. <https://doi.org/10.1016/j.mineng.2017.04.008>
- Lv W, Wang Z, Cao H, Sun Y, Zhang Y, Sun Z (2018) A critical review and analysis on the recycling of spent lithium-ion batteries. *ACS Sustain Chem Eng* 6:1504–1521. <https://doi.org/10.1021/acsschemeng.7b03811>
- Billy E, Joulié M, Laucournet R et al (2018) Dissolution mechanisms of $\text{LiNi}_{1/3}\text{Mn}_{1/3}\text{Co}_{1/3}\text{O}_2$ positive electrode material from lithium-ion batteries in acid solution. *ACS Appl Mater Interfaces* 10:16424–16435. <https://doi.org/10.1021/acsami.8b01352>
- Zhang T, He Y, Ge L et al (2013) Characteristics of wet and dry crushing methods in the recycling process of spent lithium-ion batteries. *J Power Sources* 240:766–771. <https://doi.org/10.1016/j.jpowsour.2013.05.009>
- He Y, Yuan X, Zhang G et al (2021) A critical review of current technologies for the liberation of electrode materials from foils in the recycling process of spent lithium-ion batteries. *Sci Total Environ* 766:142382. <https://doi.org/10.1016/j.scitotenv.2020.142382>
- Takacova Z, Havlik T, Kukurugya F, Orac D (2016) Cobalt and lithium recovery from active mass of spent Li-ion batteries: theoretical and experimental approach. *Hydrometallurgy* 163:9–17. <https://doi.org/10.1016/j.hydromet.2016.03.007>
- Wang X, Gaustad G, Babbitt CW (2016) Targeting high value metals in lithium-ion battery recycling via shredding and size-based separation. *Waste Manag* 51:204–213. <https://doi.org/10.1016/j.wasman.2015.10.026>
- Khoo HH (2009) Life cycle impact assessment of various waste conversion technologies. *Waste Manag* 29:1892–1900. <https://doi.org/10.1016/j.wasman.2008.12.020>
- Zhang X, Xie Y, Lin X et al (2013) An overview on the processes and technologies for recycling cathodic active materials from spent lithium-ion batteries. *J Mater Cycles Waste Manag* 15:420–430. <https://doi.org/10.1007/s10163-013-0140-y>
- Wang F, Zhang T, He Y et al (2018) Recovery of valuable materials from spent lithium-ion batteries by mechanical separation and thermal treatment. *J Clean Prod* 185:646–652. <https://doi.org/10.1016/j.jclepro.2018.03.069>
- Liu C, Lin J, Cao H et al (2019) Recycling of spent lithium-ion batteries in view of lithium recovery: a critical review. *J Clean Prod* 228:801–813. <https://doi.org/10.1016/j.jclepro.2019.04.304>
- Burat F, Baştürkücü H, Özer M (2019) Gold&silver recovery from jewelry waste with combination of physical and physicochemical methods. *Waste Manag* 89:10–20. <https://doi.org/10.1016/j.wasman.2019.03.062>
- Diñç Nİ, Tosun AU, Baştürkücü E, Özer M, Burat F (2022) Recovery of valuable metals from WPCB fines by centrifugal gravity separation and froth flotation. *J Mater Cycles Waste Manag* 24:224–236. <https://doi.org/10.1007/s10163-021-01310-8>
- Sommerville R, Zhu P, Rajaeifar MA, Heidrich O, Goodship V, Kendrick E (2021) A qualitative assessment of lithium ion battery recycling processes. *Resour Conserv Recycl* 165:105219. <https://doi.org/10.1016/j.resconrec.2020.105219>
- Tanışal E, Özer M, Burat F (2020) Precious metals recovery from waste printed circuit boards by gravity separation and leaching. *Miner Process Extr* 42:24–37. <https://doi.org/10.1080/08827508.2020.1795849>
- Zhang G, He Y, Wang H, Feng Y, Xie W, Zhu X (2019) Application of mechanical crushing combined with pyrolysis-enhanced flotation technology to recover graphite and LiCoO_2 from spent lithium-ion batteries. *J Clean Prod* 231:1418–1427. <https://doi.org/10.1016/j.jclepro.2019.04.279>
- Güney A, Özdilek C, Kangal MO, Burat F (2015) Flotation characterization of PET and PVC in the presence of different plasticizers. *Sep Purif Technol* 151:47–56. <https://doi.org/10.1016/j.seppur.2015.07.027>
- Vanderbruggen A, Salces A, Ferreira A et al (2022) Improving separation efficiency in end-of-life lithium-ion batteries flotation using attrition pre-treatment. *Minerals* 12:72. <https://doi.org/10.3390/min12010072>
- Yenial Ü, Burat F, Yüce AE et al (2013) Separation of PET and PVC by flotation technique without using alkaline treatment. *Miner Process Extr* 34:412–421. <https://doi.org/10.1080/08827508.2012.702705>
- Meshram P, Mishra A, Abhilash SR (2020) Environmental impact of spent lithium ion batteries and green recycling perspectives by organic acids—a review. *Chemosphere* 242:125291. <https://doi.org/10.1016/j.chemosphere.2019.125291>
- Prasetyo E, Muryanta WA, Anggraini AG, Sudibyo S, Amin M, Muttaqii MA (2022) Tannic acid as a novel and green leaching reagent for cobalt and lithium recycling from spent lithium-ion

- batteries. *J Mater Cycles Waste Manag* 24:927–938. <https://doi.org/10.1007/s10163-022-01368-y>
27. Contestabile M, Panero S, Scrosati B (2001) A laboratory-scale lithium-ion battery recycling process. *J Power Sources* 92:65–69. [https://doi.org/10.1016/S0378-7753\(00\)00523-1](https://doi.org/10.1016/S0378-7753(00)00523-1)
 28. Zhang P, Yokoyama T, Itabashi O, Suzuki TM, Inoue K (1998) Hydrometallurgical process for recovery of metal values from spent lithium-ion secondary batteries. *Hydrometallurgy* 47:259–271. [https://doi.org/10.1016/S0304-386X\(97\)00050-9](https://doi.org/10.1016/S0304-386X(97)00050-9)
 29. Shin SM, Kim NH, Sohn JS, Yang DH, Kim YH (2005) Development of a metal recovery process from Li-ion battery wastes. *Hydrometallurgy* 79:172–181. <https://doi.org/10.1016/j.hydromet.2005.06.004>
 30. Aktas S, Fray DJ, Burheim O, Fenstad J, Açma E (2006) Recovery of metallic values from spent Li ion secondary batteries. *Trans Inst Min Metallur Sect C Miner Process Extr* 115:95–100. <https://doi.org/10.1179/174328506X109040>
 31. Dorella G, Mansur MB (2007) A study of the separation of cobalt from spent Li-ion battery residues. *J Power Sources* 170:210–215. <https://doi.org/10.1016/j.jpowsour.2007.04.025>
 32. Swain B, Jeong J, Lee JC, Lee GH, Sohn JS (2007) Hydrometallurgical process for recovery of cobalt from waste cathodic active material generated during manufacturing of lithium ion batteries. *J Power Sources* 167:536–544. <https://doi.org/10.1016/j.jpowsour.2007.02.046>
 33. Lee CK, Rhee K-I (2003) Reductive leaching of cathodic active materials from lithium ion battery wastes. *Hydrometallurgy* 68:5–10. [https://doi.org/10.1016/S0304-386X\(02\)00167-6](https://doi.org/10.1016/S0304-386X(02)00167-6)
 34. Li L, Ge J, Wu F, Chen R, Chen S, Wu B (2010) Recovery of cobalt and lithium from spent lithium ion batteries using organic citric acid as leachant. *J Hazard Mater* 176:288–293. <https://doi.org/10.1016/j.jhazmat.2009.11.026>
 35. Li L, Ge J, Chen R, Wu F, Chen S, Zhang X (2010) Environmental friendly leaching reagent for cobalt and lithium recovery from spent lithium-ion batteries. *Waste Manag* 30:2615–2621. <https://doi.org/10.1016/j.wasman.2010.08.008>
 36. de Oliveira DJ, Stefanello Cadore J, da Silveira de Oliveira F, Tanabe EH, Bertuol DA (2019) Recovery of metals from spent lithium-ion batteries using organic acids. *Hydrometallurgy* 190:105169. <https://doi.org/10.1016/j.hydromet.2019.105169>
 37. Chen WS, Ho HJ (2018) Recovery of valuable metals from lithium-ion batteries NMC cathode waste materials by hydrometallurgical methods. *Metals* 8:321. <https://doi.org/10.3390/met8050321>
 38. Takahashi VCI, Botelho Junior AB, Espinosa DCR, Tenório JAS (2020) Enhancing cobalt recovery from Li-ion batteries using grinding treatment prior to the leaching and solvent extraction process. *J Environ Chem Eng* 8:103801. <https://doi.org/10.1016/j.jece.2020.103801>
 39. Meshram P, Pandey BD, Mankhand TR (2015) Hydrometallurgical processing of spent lithium ion batteries (LIBs) in the presence of a reducing agent with emphasis on kinetics of leaching. *J Chem Eng* 281:418–427. <https://doi.org/10.1016/j.cej.2015.06.071>
 40. Swain B (2017) Recovery and recycling of lithium: A review. *Sep Purif Technol* 172:388–403. <https://doi.org/10.1016/j.seppur.2016.08.031>
 41. Chen X, Xu B, Zhou T, Liu D, Hu H, Fan S (2015) Separation and recovery of metal values from leaching liquor of mixed-type of spent lithium-ion batteries. *Sep Purif Technol* 144:197–205. <https://doi.org/10.1016/j.seppur.2015.02.006>
 42. Pant D, Dolker T (2017) Green and facile method for the recovery of spent Lithium Nickel Manganese Cobalt Oxide (NMC) based Lithium ion batteries. *Waste Manag* 60:689–695. <https://doi.org/10.1016/j.wasman.2016.09.039>
 43. Nan J, Han D, Zuo X (2005) Recovery of metal values from spent lithium-ion batteries with chemical deposition and solvent extraction. *J Power Sources* 152:278–284. <https://doi.org/10.1016/j.jpowsour.2005.03.134>
 44. Wang HY, Huang K, Zhang Y, Chen X, Jin W, Zheng SL, Zhang Y, Li P (2017) Recovery of lithium, nickel, and cobalt from spent lithium-ion battery powders by selective ammonia leaching and an adsorption separation system. *ACS Sustain Chem Eng* 5:11489–11495. <https://doi.org/10.1021/acssuschemeng.7b02700>
 45. Zhang W, Cheng CY (2007) Manganese metallurgy review. Part II: Manganese separation and recovery from solution. *Hydrometallurgy* 89:160–177. <https://doi.org/10.1016/j.hydromet.2007.08.009>
 46. Chagnes A, Pospiech B (2013) A brief review on hydrometallurgical technologies for recycling spent lithium-ion batteries. *J Chem Technol Biotechnol* 88:1191–1199. <https://doi.org/10.1002/jctb.4053>
 47. Mennik F, Dinç Nİ, Burat F (2023) Selective recovery of metals from spent mobile phone lithium-ion batteries through froth flotation followed by magnetic separation procedure. *Results Eng* 17:100868. <https://doi.org/10.1016/j.rineng.2022.100868>
 48. Burat F, Demirağ A, Şafak MC (2020) Recovery of noble metals from floor sweeping jewelry waste by flotation-cyanide leaching. *J Mater Cycles Waste Manag* 22:907–915. <https://doi.org/10.1007/s10163-020-00982-y>
 49. Fadel MA, Kamel NA, Darwish MM, El-Messieh SL, Abd-El-Nour K, Khalil WA (2020) Preparation and characterization of polyethylene terephthalate–chamomile oil blends with enhanced hydrophilicity and anticoagulant properties. *Prog Biomater* 9:97–106. <https://doi.org/10.1007/s40204-020-00133-4>
 50. Saneie R, Abdollahi H, Ghassa S, Azizi D, Chelgani SC (2022) Recovery of copper and aluminum from spent lithium-ion batteries by froth flotation: a sustainable approach. *J Sustain Metall* 8:386–397. <https://doi.org/10.1007/s40831-022-00493-0>
 51. He LP, Sun SY, Mu YY, Song XF, Yu JG (2017) Recovery of lithium, nickel, cobalt, and manganese from spent lithium-ion batteries using l-tartaric acid as a leachant. *ACS Sustain Chem Eng* 5:714–721. <https://doi.org/10.1021/acssuschemeng.6b02056>
 52. Pinna EG, Toro N, Gallegos S, Rodriguez MH (2022) A novel recycling route for spent li-ion batteries. *Materials* 15:44. <https://doi.org/10.3390/ma15010044>
 53. Kang J, Senanayake G, Sohn J, Shin SM (2010) Recovery of cobalt sulfate from spent lithium ion batteries by reductive leaching and solvent extraction with Cyanex 272. *Hydrometallurgy* 100:168–171. <https://doi.org/10.1016/j.hydromet.2009.10.010>
 54. Lain MJ (2001) Recycling of lithium ion cells and batteries. *J Power Sources* 97–98:736–738. [https://doi.org/10.1016/S0378-7753\(01\)00600-0](https://doi.org/10.1016/S0378-7753(01)00600-0)
 55. Lee CK, Rhee K-I (2002) Preparation of LiCoO₂ from spent lithium-ion batteries. *J Power Sources* 109:17–21. [https://doi.org/10.1016/S0378-7753\(02\)00037-X](https://doi.org/10.1016/S0378-7753(02)00037-X)
 56. Guimarães LF, Botelho Junior AB, Espinosa DCR (2022) Sulfuric acid leaching of metals from waste Li-ion batteries without using reducing agent. *Miner Eng* 183:107597. <https://doi.org/10.1016/j.mineng.2022.107597>

Publisher's Note Springer Nature remains neutral with regard to jurisdictional claims in published maps and institutional affiliations.

Springer Nature or its licensor (e.g. a society or other partner) holds exclusive rights to this article under a publishing agreement with the author(s) or other rightsholder(s); author self-archiving of the accepted manuscript version of this article is solely governed by the terms of such publishing agreement and applicable law.